# Fracture Toughness of Ti-6Al-4V after Welding and Postweld Heat Treatment

*Weld metal fracture is related to the thickness and morphology of grain boundary alpha and intragranular alpha*

BY K. KESHAVA MURTHY AND S. SUNDARESAN

ABSTRACT. The fracture toughness ($J_{IC}$) of the fusion zone of Ti-6Al-4V alloy welds was studied in terms of microstructural changes in the as-welded condition and following postweld heat treatment. Gas tungsten arc and electron beam welds were produced in sheet material over a limited range of heat input and subsequently heat treated at 700°C (1290°F) and 900°C (1650°F). In the as-welded condition, the weld microstructure was a mixture of diffusional and martensitic alpha phases, whose proportion varied with heat input and cooling rate. The fusion zone exhibited low ductility resulting from the highly acicular microstructure and a large prior-beta grain size. Postweld heat treatment tempered the martensite and coarsened the microstructure, but a beneficial effect on ductility was realized only after treatment at 900°C. Fracture toughness in the as-welded condition was greater than for the base metal and was attributed to the lamellar microstructure of the fusion zone and absence of continuous alpha film along the grain boundaries. Postweld heat treatment at 700°C reduced the fracture toughness considerably and, as in the case of ductility, it was necessary to heat treat at 900°C to produce an improvement. These variations in fracture toughness correlated well with fractographic features and, in terms of the microstructure, were found to be related to the coarseness of the transformed/ aged beta matrix and to the thickness and morphology of the alpha phase formed at the grain boundaries.

## Introduction

It has long been known that welding of alpha-beta titanium alloys results in a reduction in ductility of the fusion zone, even though there is no adverse effect on strength, which, in fact, may increase (Ref. 1). Much effort has been directed toward improving tensile elongation through changes in weld energy input (Ref. 2) and postweld heat treatment (Ref. 3). The improvement of ductility in a dissimilar titanium alloy weld has also recently been discussed (Ref. 4). Of late, there is growing concern that rapid cooling during welding may also reduce fracture toughness in the fusion zone of welded structural components in titanium alloys. With the increasing use of structural design based upon fracture mechanics criteria (Ref. 5), there is a greater need to develop a fundamental metallurgical understanding of the effects of welding procedures to obtain adequate fracture toughness without compromising strength levels.

A great variety of microstructures can be produced in alpha-beta titanium alloys by introducing variations in thermal and mechanical history, thus implying that their fracture toughness can also be made to vary widely, and that their dependence on the processing route could be complex. Such dependence has been the subject of many investigations in the past (Refs. 6–8). These studies have provided clear indications of the superiority of microstructures that contain a large percentage of acicular alpha. This has been related, in the case of transgranular fracture, to the morphological characteristics of the acicular alpha phase (Ref. 9). These platelets, with their high aspect ratios, provide extended alpha-beta interfaces for preferential crack propagation. The many changes of crack direction, as these interfaces are followed, result in greater energy consumption. In the case of intergranular fracture, on the other hand, high fracture toughness has been attributed to increased fracture path lengths as the crack follows prior-beta grain boundaries (Ref. 10). Structures containing grain boundary alpha are particularly susceptible to intergranular fracture. The thickness of the grain boundary alpha layer then becomes important to determining toughness. It has been found, for example, that as the alpha thickness increased, greater energy was absorbed (Ref. 11). This has been explained in terms of the increased plastic flow of the thicker alpha layer, which is effectively less constrained by the harder surrounding transformed-beta matrix. It has been suggested, however, that as the grain boundary alpha phase becomes coarse, there might be little difference between the alpha phase/matrix interfaces at the grain boundaries and those within the grains. In this case, there would be no preference for grain boundary void formation and intergranular fracture (Ref. 12).

Although fracture toughness has been widely studied as a function of thermal and mechanical processing conditions of the base material, there have been relatively fewer investigations in respect to welded joints. In general, it has been found that very fine microstructures produced during welding result in low fracture toughness, and that postweld heat treatment improves fracture toughness

**KEY WORDS**

Titanium Alloys
GTA Welding
EB Welding
Postweld Annealing
Microstructure
Fracture Toughness
Fractography

*K. KESHAVA MURTHY is Research Scholar and S. SUNDARESAN is Professor at the Department of Metallurgical Engineering, Indian Institute of Technology, Madras, India.*

by coarsening the microstructure. Working with simulated heat-affected zones as well as actual weldment fusion zones of a Ti-6Al-6V-2Sn alloy, Wu (Ref. 13) reported a reduction in fracture toughness as the cooling rate was increased, and attributed this reduction to an increase in the percentage of the martensitic alpha prime phase and a decrease in the diffusional alpha platelet size produced. The toughness was not affected by the amount of beta phase present. Postweld heat treatment at temperatures greater than 760°C (1400°F) raised fracture toughness by reducing the alpha prime fraction and coarsening the structure. The use of a relatively slow weldment cooling rate as a means of improving fracture toughness has been recommended (Ref. 14), particularly for those alloys that form orthorhombic martensite when cooled rapidly. It was found that, in a Ti-4.5Al-5Mo-1.5Cr alloy, "optimized" electron beam welding produced fusion zone regions characterized by low fracture toughness caused by an extremely fine alpha-beta microstructure, and that toughness and ductility could be improved by postweld heat treatment that coarsened the microstructure. Much Russian work has been reported where Charpy impact toughness of the weld metal was used along with other mechanical properties to optimize welding and postweld heat treatment parameters in several titanium alloys (Refs. 15–17). However, no correlation of toughness with any microstructural feature was described. In one of the very few investigations where $K_{IC}$ was determined, it was suggested that, to raise fracture toughness, the postweld heat treatment temperature must be higher than that required for stress relief and restoration of ductility (Ref. 18).

The current study reports work directed toward determining the relationship between fracture toughness of the weld metal in an alpha-beta titanium alloy to its microstructural condition; specifically, the microstructural variations were produced in Ti-6Al-4V alloy by using different weld energy inputs and by heat treating after welding at two different temperatures. The effect of the microstructural features on mechanical properties, particularly on fracture toughness, has been studied in detail.

## Experimental Work

The work was carried out on 6-mm (15/64-in.) thick alpha-beta processed Ti-6Al-4V sheet with a chemical composition (actual for this alloy heat) of: Al–6.01; V–4.01; C–0.01, Cr–0.14; Fe–0.13; H–0.008; O–0.11; N–0.004; Ti–balance (all weight percentages).

Three welding processes were used: 1) manual gas tungsten arc welding (M-GTAW) in a 1.5-m-diameter hemispherical glovebox filled with argon; 2) automatic gas tungsten arc welding (A-GTAW) with auxiliary trailing and backing gas shields; and 3) electron beam welding (EBW) in a chamber with a vacuum of $10^{-5}$ torr. The welding parameters are listed in Table 1. Autogenous, complete joint penetration, bead-on-plate welds were made in all cases. In both M-GTAW and A-GTAW, two passes were deposited, one on each side. Just prior to welding, the strips were pickled in a $HF/HNO_3$ solution and degreased with acetone. Postweld heat treatment was performed at 900°C and at 700°C. The former was selected because an earlier report (Ref. 19) had indicated that a high-temperature treatment was required to ensure adequate ductility. Postweld heat treatment was also done at 700°C to follow the structural changes progressively and to see if improvement over the as-welded condition could be noted. The duration of heat treatment was four hours, which was followed by furnace cooling. All heat treatments were carried out in a vacuum furnace at a pressure of $10^{-5}$ torr.

Preliminary evaluation of the joints was carried out by longitudinal all-weld tensile testing (Table 2) and hardness surveys across the weld. In tensile specimens from electron beam welded strips, 80% of the width in the gauge-length portion was comprised of the weld metal. The structural changes were followed through light microscopy and transmission electron microscopy. For the former, a $HF/HNO_3$ etch was employed. Thin foils for TEM were prepared by twin jet electropolishing, using a solution containing 5% sulphuric acid and 95% methanol at a temperature of –40°C (–40°F).

As a measure of fracture toughness, the elastic-plastic parameter $J_{IC}$ was used, since the small thickness of the sheet material precluded the application of linear elastic fracture mechanics. The tests were performed in accordance with ASTM E813-89 (Ref. 20). Single-edged notched compact tension specimens

**Table 1 — Welding Parameters for Manual GTA, Automatic GTA, and Electron Beam Welding of Ti-6Al-4V**

| Process | Arc/Beam Voltage (V) | Arc/Beam Current (A) | Travel Speed (mm/s) | Heat Input (J/mm) |
|---|---|---|---|---|
| EBW | $100 \times 10^3$ | $63 \times 10^{-3}$ | 20 | 315 |
| Automatic GTAW | 12 | 200 | 5 | 480 |
| Manual GTAW | 14 | 220 | 4.6 | 670 |

Other Parameters

| | |
|---|---|
| Electron beam welding: | Vacuum of $10^{-5}$ torr |
| Automatic GTAW: | Torch gas flow rate = 7 L/min |
| | Trailing gas flow rate = 14 L/min |
| | Backing gas flow rate = 5 L/min |
| Manual GTAW: | Torch gas flow rate = 15 L/min |

**Table 2 — Fusion Zone Tensile Properties of Ti-6Al-4V Weldments**

| Process | Conditions | Yield Strength (MPa) | Ultimate Tensile Strength (MPa) | Elongation (%) |
|---|---|---|---|---|
| EBW | As-welded | 894 | 1005 | 9.5 |
| | After PWHT at 700°C | 884 | 997 | 8 |
| | After PWHT at 900°C | 805 | 936 | 12 |
| Automatic GTAW | As-welded | 880 | 975 | 8 |
| | After PWHT at 700°C | 870 | 960 | 6.5 |
| | After PWHT at 900°C | 784 | 896 | 12.5 |
| Manual GTAW | As-welded | 873 | 986 | 8.5 |
| | After PWHT at 700°C | 866 | 965 | 6.5 |
| | After PWHT at 900°C | 800 | 925 | 12 |

Notes:
1) PWHT stands for postweld heat treatment.
2) All results are an average of two tests each.
3) For comparison, the base metal properties were: 857 Mpa (YS), 973 MPa (UTS) and 14.5% (elongation).

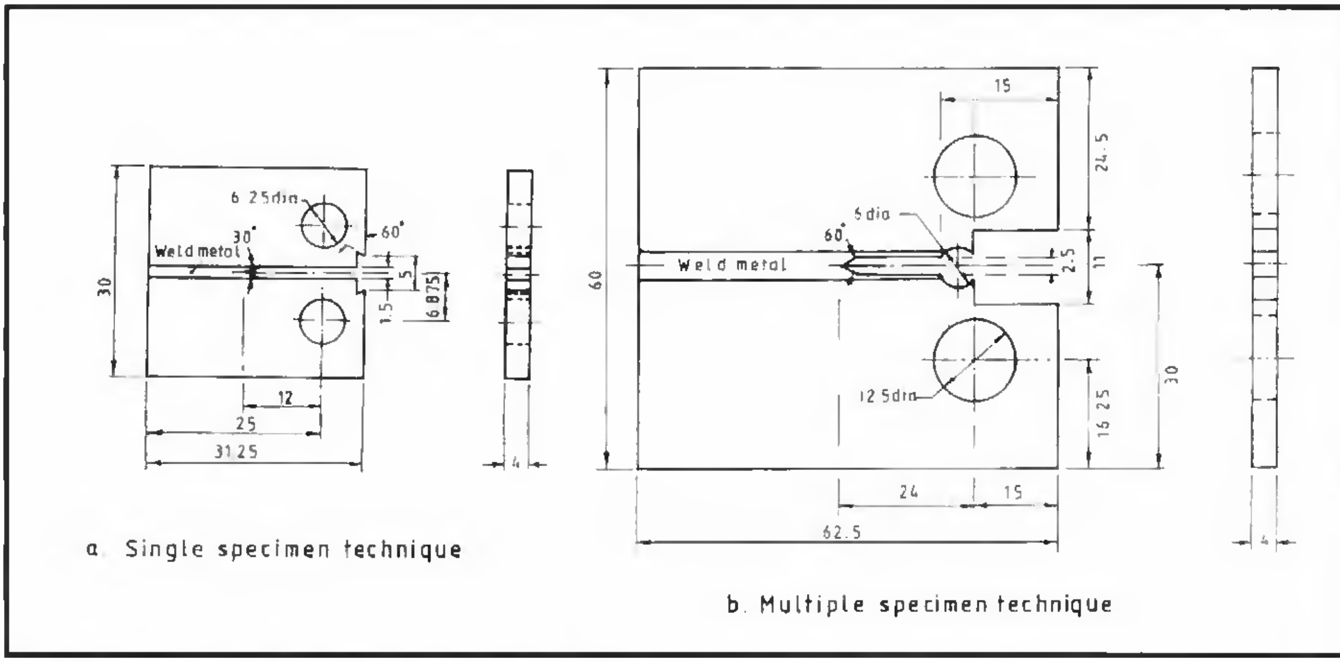


*Fig. 1 — Compact tension specimen for fracture toughness tests.*

with the geometry shown in Fig. 1 were used. The notch was centered in the weld deposit and oriented such that the crack propagated along the weld. In the first series, the multiple specimen technique was employed. Since some of the fracture toughness values so determined were somewhat unexpected, confirmatory tests were also performed using the single specimen technique. Fatigue precracking and subsequent loading for crack extension were carried out in a 100 kN servohydraulic testing machine. A plot of J-integral (determined from specimen dimensions and load vs. load line displacement records) vs. crack extension Δ a (measured after heat tinting and crack opening in the multiple specimen technique and determined using an elastic compliance procedure in the single specimen method) enabled the estimation of $J_{IC}$. Representative J–Δ a curves for each technique are shown in Figs. 2 and 3. After $J_{IC}$ testing, the fracture surfaces were examined using a scanning electron microscope.

The fracture toughness values are listed in Table 3. In the multiple specimen method, for each welded or postweld treated condition, seven or eight specimens on the average were tested, in order to get at least four J–Δ a data points between the two exclusion lines drawn parallel to the blunting line at Δ a = 0.15 mm and at Δ a = 1.5 mm — Fig. 2. In the single specimen technique, the objective was to ensure that, in at least one specimen, the crack was confined entirely to the weld metal and propagated nearly parallel to the welding direction. This

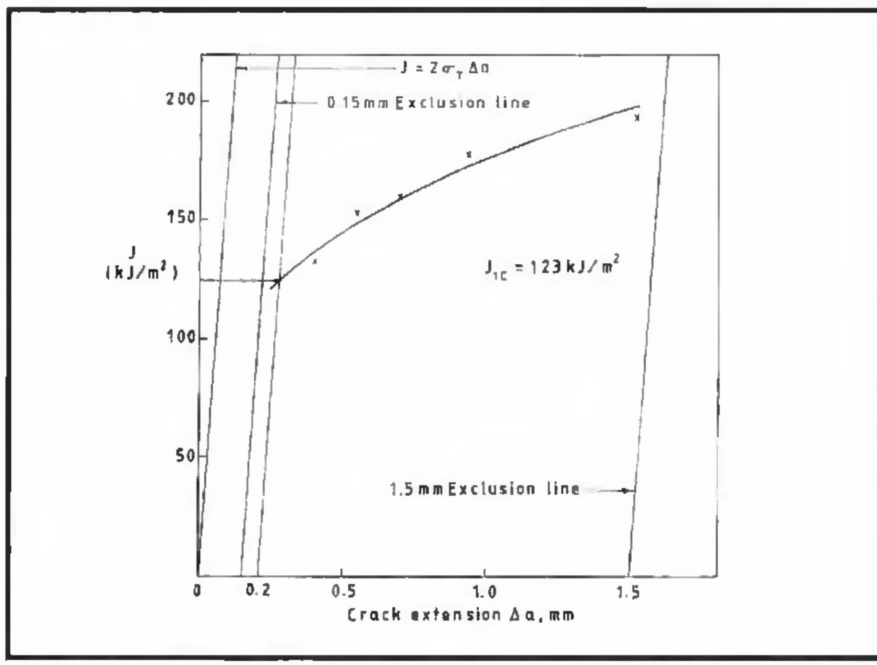


*Fig. 2 — $J_R$ curve for Ti-6Al-4V manual GTA weld, postweld heat treated at 900°C — multiple specimen technique.*

**Table 3 — Fusion Zone Fracture Toughness of Ti-6Al-4V Weldments**

| Process | $J_{IC}$ (kJ/m²) Single Specimen Technique | | | $J_{IC}$ (kJ/m²) Multiple Specimen Technique | | |
|---|---|---|---|---|---|---|
| | As-welded | PWHT 700°C | PWHT 900°C | As-welded | PWHT 700°C | PWHT 900°C |
| EBW | 100 | 44 | 125 | 79 | 67 | 126 |
| Automatic GTAW | 96 | 50 | 107 | 98 | 54 | 124 |
| Manual GTAW | 91 | 53 | 110 | 97 | 55 | 123 |

Base metal fracture toughness: 68 kJ/m² (single specimen technique)
74 kJ/m² (multiple specimen technique)

Note: See text for number of specimens tested in each condition.

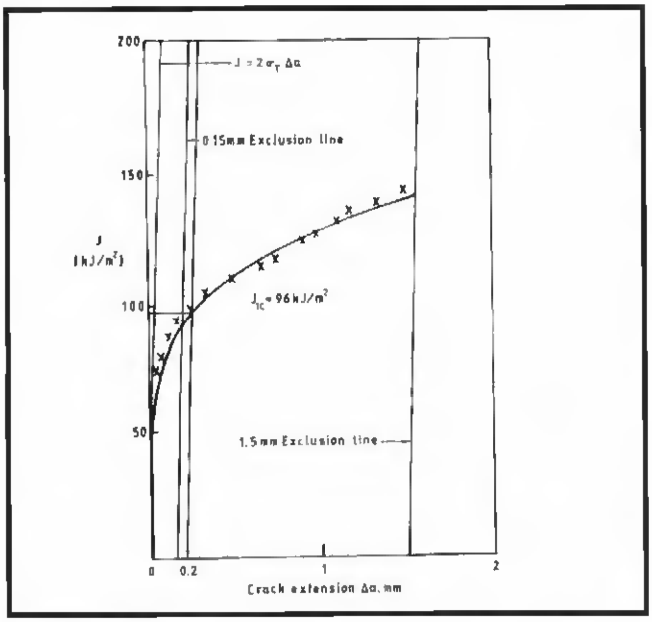


Fig. 3 — $J_R$ curve for Ti-6Al-4V automatic GTA weld, as-welded — single-specimen technique.

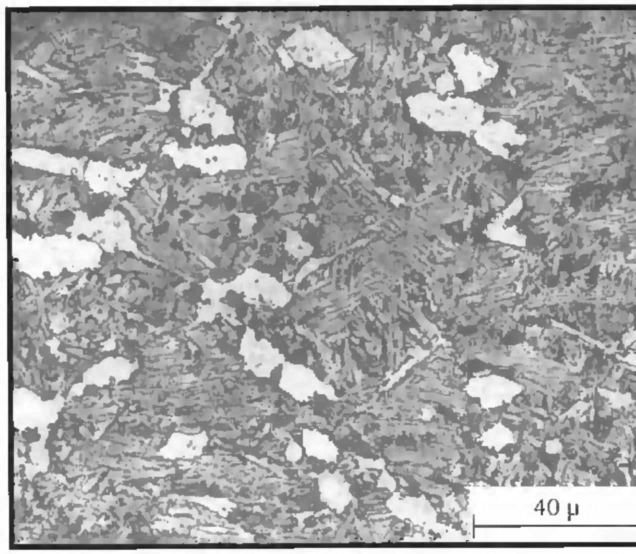


Fig. 4 — Light micrograph of the base metal. Arrow A — Primary alpha; Arrow B — Transformed-beta.

necessitated, in many cases, the testing of at least two specimens; in electron beam welds, where the crack often tended to run out of the fusion zone, many more specimens were required. Table 3 reports values from welded specimens in which the crack propagated entirely within the weld metal and parallel to its length.

## Results and Discussion

### Structural Features

The base metal microstructure seen in Fig. 4 shows a mixture of primary, globular alpha grains in a transformed-beta matrix. In the as-welded condition, the fusion zone exhibited a fine acicular microstructure for all three welding conditions. This is shown in Fig. 5 for EB and M-GTA welds. The slight intragranular coarsening observed in the GTA weld metal is a result of the relatively slower cooling in this process as compared to EBW. The presence of an unresolved region near the prior-beta grain boundary triple point suggests the formation of the diffusional alpha phase at the grain boundary. However, it may be noted that the grain boundary alpha phase is not continuous. The difference between EB and GTA welds is also revealed in the electron micrographs shown in Fig. 6. The former is almost entirely martensitic, the structure consisting of large primary plates with partitioned regions containing smaller secondary plates of varying orientation. The slower cooled gas tungsten arc weld fusion zone, on the other hand, exhibits a mixture of martensite and a colony structure comprised of alpha plates separated by thin strips of retained beta. The presence of the beta phase, revealed by

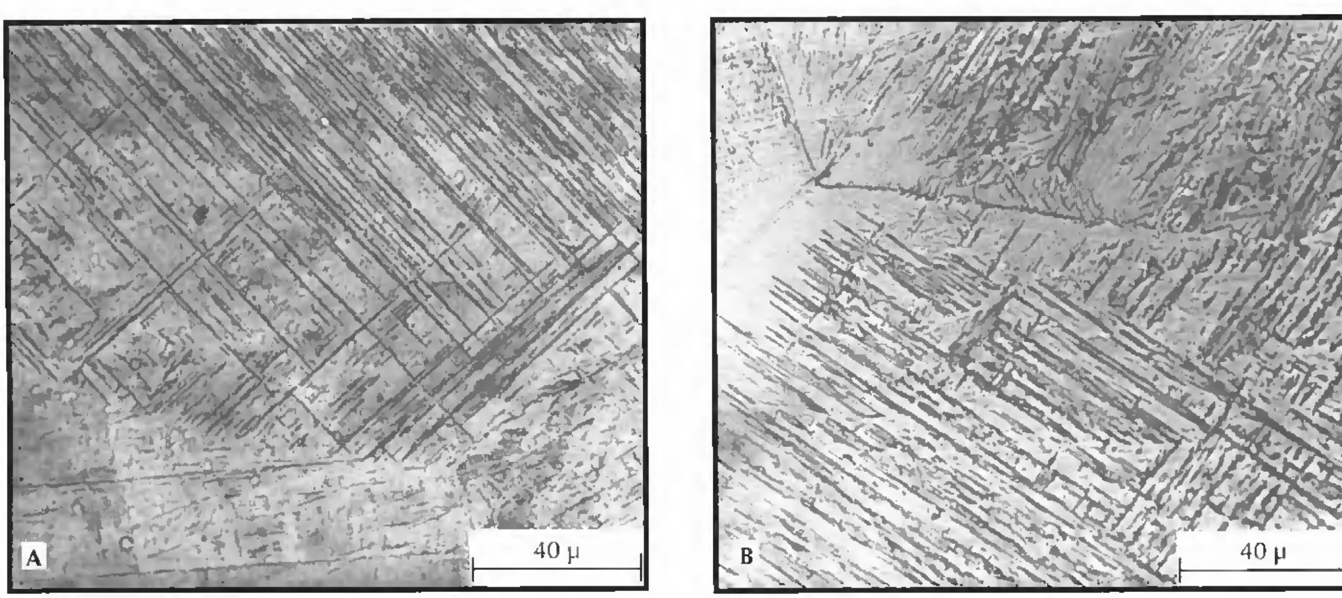


Fig. 5 — Light micrographs of fusion zone, as-welded condition. A — Electron beam weld; arrow indicates prior-beta grain boundary; B — manual GTA weld; arrow shows unresolved region near grain boundary triple point.

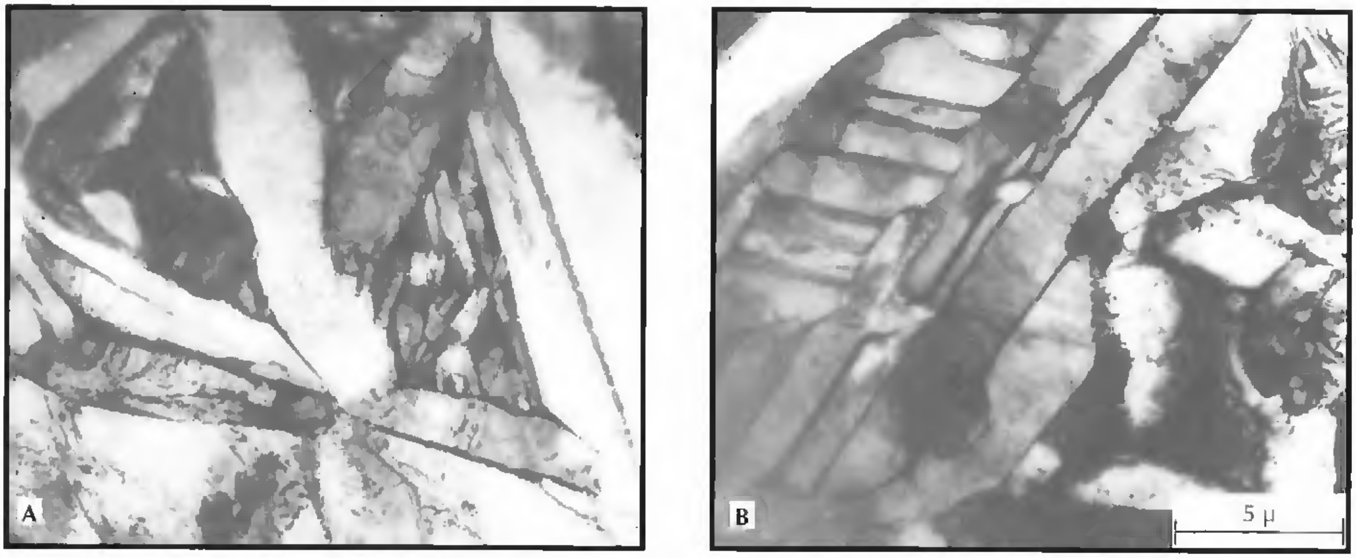


Fig. 6 — Transmission electron micrographs of fusion zone, as-welded condition. A — Electron beam weld, M — martensite plate; B — manual GTA weld, M — martensite plate; arrow shows colony product.

selected area diffraction, confirms the occurrence of the diffusional transformation, because such formation of the alpha phase is necessary to enrich the remaining beta and lower the Ms temperature. The as-welded microstructure of the A-GTA welded fusion zone showed features intermediate to those of EB and M-GTA welds.

The differences in the as-welded condition, however, are eliminated by postweld heat treatment, during which the material seeks to attain thermodynamic equilibrium. It is known that during such heat treatment the following events could occur: 1) formation of beta from martensite whose composition thus approaches that of equilibrium alpha; and 2) precipitation of alpha in any retained beta (Ref. 3). Higher temperatures and longer times would promote overaging and grain coarsening effects. Figures 7 and 8 show the microstructures of M-GTA welds after postweld heat treatment at 700°C and 900°C, respectively. Similar structures were obtained in the case of postweld heat treated EB and A-GTA welds. Postweld heat treatment at 700°C has resulted in an alpha-beta basketweave structure which has not coarsened as much as it had after the treatment at 900°C. The thin alpha film outlining the prior beta grain boundaries can also be noticed in Fig. 7. The structure after the 900°C treatment shows a typical basketweave pattern of thick lenticular alpha plates in a beta matrix. The grain boundary alpha phase, which is discontinuous and exhibits a globular morphology in some places, is thicker and more conspicuously developed at 900°C than at 700°C. It is interesting to note that, even at 900°C, there is no globularization of the intragranular alpha phase and the lath appearance is still retained. A comparison of transmission electron micrographs after postweld heat treatment at 700°C (Fig. 9) and 900°C (Fig. 10) clearly reveals the difference in alpha plate growth at the two temperatures. While the parallel plate colony structure

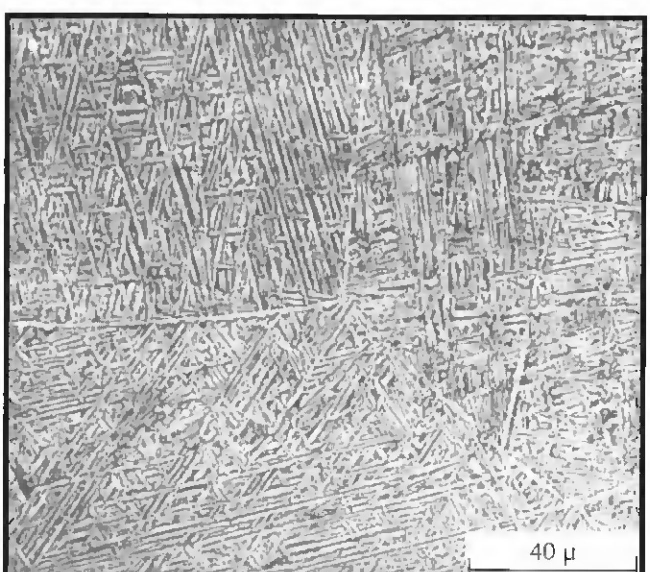


Fig. 7 — Light micrograph of M-GTA weld metal after postweld heat treatment at 700°C. Arrow shows thin alpha layer outlining grain boundary.

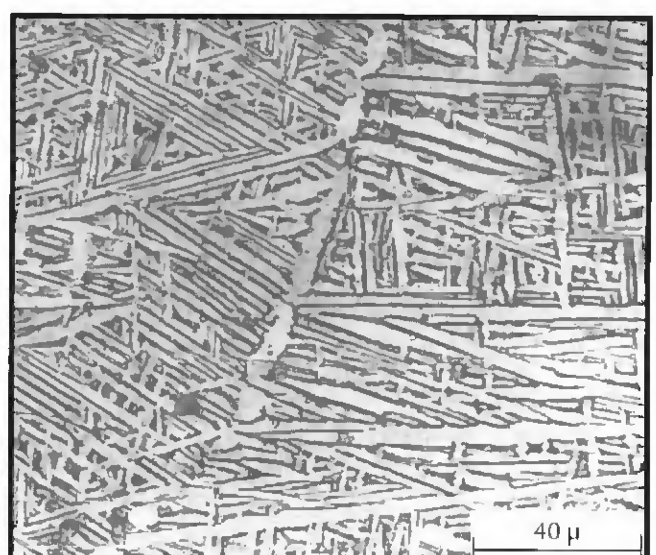


Fig. 8 — Light micrograph of M-GTA weld metal after postweld heat treatment at 900°C. Arrow indicates thick, discontinuous alpha at grain boundary.

of alpha plates separated by layers of beta is fully developed at 900°C, it occurs only partially after the 700°C treatment. As evidence for the incomplete reaction at 700°C, some of the plates of martensite may still be observed in Fig. 9. In contrast, after the treatment at 900°C, Fig. 10 shows that the alpha plates are essentially free from dislocation substructures.

A point of further interest is that the differences in microstructure noted in the as-welded condition were completely eliminated at the end of either of the postweld heat treatments.

## Tensile and Hardness Tests

The tensile test results are listed in Table 2. Considering the as-welded condition, the yield and ultimate tensile strengths of the fusion zone are slightly higher than for the base material. This is accompanied, however, by a significant reduction in ductility as a result of welding. The tensile elongation drops from 14.5% in the base material to values ranging from 8–9.5% in the fusion zone. The reduction in as-welded ductility is attributable to the coarse prior-beta grain size and the high aspect ratio, transformed-beta microstructure. The increased yield strength of the weld metal is presumably a consequence of the presence of martensite and the fineness of the acicular, intragranular microstructure. A high yield strength is known to characterize fine precipitated alpha structures in general (Ref. 7) and, in weldments, fine, predominantly alpha-prime microstructures (Ref. 1). As the microstructure coarsens, owing to a reduced weld cooling rate, intragranular slip becomes easier and the strength decreases (Ref. 1). A trend may be noticed in Table 2 for the yield strength to be slightly reduced as a cooling rate decreases from EBW through A-GTAW to M-GTAW. It must be mentioned, however, that the difference in tensile properties among the three welding processes employed is not considerable. One reason for this is that the range of heat inputs used in this study (315–670 J/mm) was not very wide.

Table 2 shows that a postweld heat treatment at 700°C is not beneficial from the standpoint of ductility. In fact, it is found to lead to a slight reduction in tensile elongation from the as-welded condition. Only a heat treatment at 900°C is able to raise the ductility to a value comparable to that of the base material. The yield and ultimate tensile strengths are lowered by postweld heat treatment, particularly at 900°C, but the extent of the reduction is not significant.

The hardness variations across the A-GTA weld in the as-welded and heat treated conditions are shown in Fig. 11. Similar distributions were obtained in the case of EB and M-GTA welds. The hardening of the weld zone with peaking at its center is attributable to the difficulty of slip in the extremely fine, lamellar intragranular microstructure. This conforms with the increase in yield strength of the fusion zone as a result of welding. On traversing away from the weld center into the heat-affected zone, the cooling rate decreases. As discussed above for yield strength, this coarsens the structure and reduces strength and hardness. Coarsening also occurs during postweld annealing, which results in softening as seen in

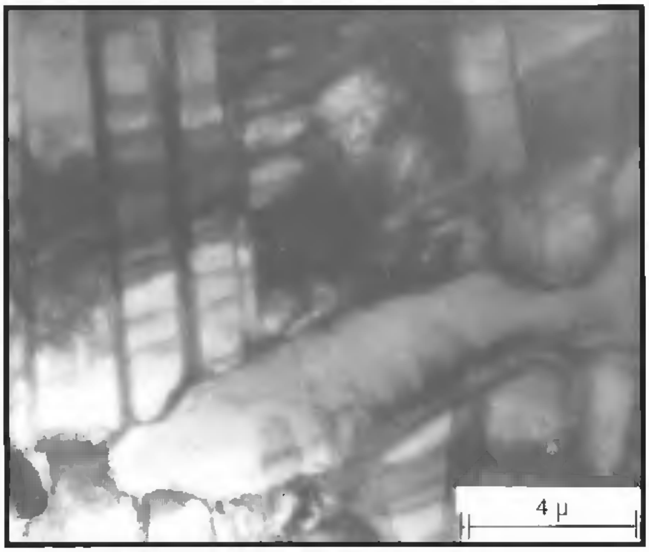


*Fig. 9 — Transmission electron micrograph of M-GTA weld metal after postweld heat treatment at 700°C. M — martensite plate.*

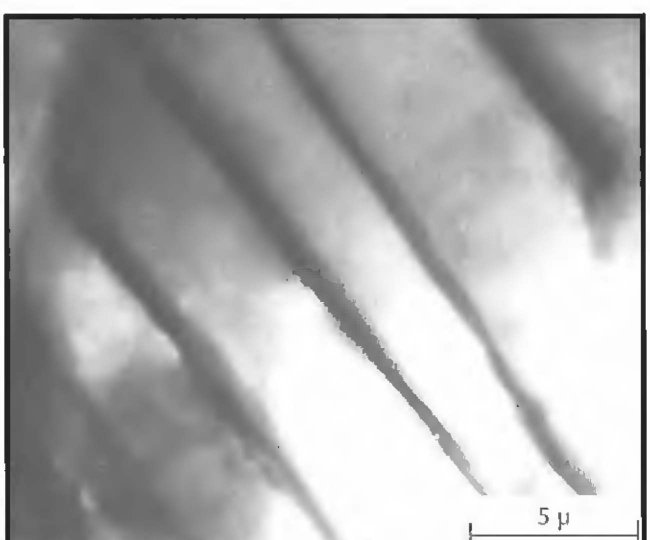


*Fig. 10 — Transmission electron micrograph of M-GTA weld metal after postweld heat treatment at 900°C. α — Colony alpha plates; arrow shows beta layer.*

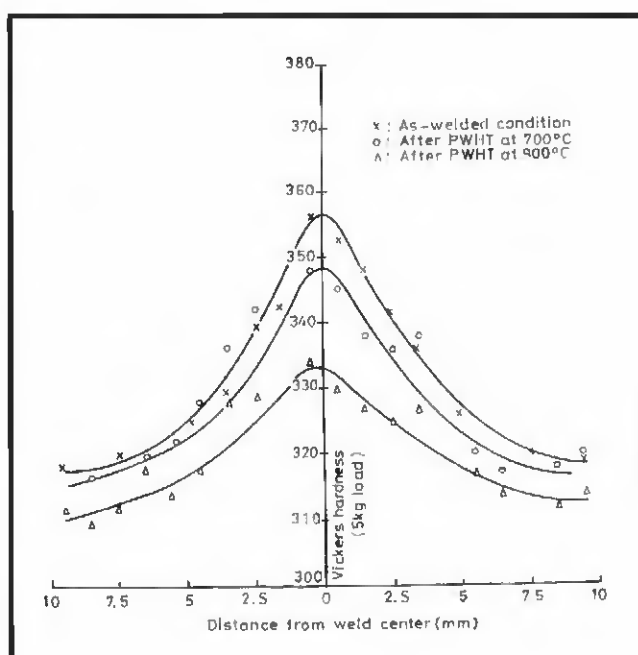


*Fig. 11 — Hardness variation across automatic GTA weld.*

Fig. 11. It may be observed, however, that postweld heat treatment at 700°C has not led to a substantial reduction in hardness. The softening is much more pronounced at 900°C.

The poor ductility after the 700°C treatment is probably a result of the fact that the microstructure has not sufficiently coarsened at this temperature and continues to exhibit a high aspect ratio of the alpha plates present. It is known that under such conditions, tensile fracture strain is low, since a greater alpha-beta interfacial area per unit volume is available for void nucleation (Ref. 7). As Fig. 9 shows, the tempering of martensite is not yet complete at 700°C. A nearly dislocation free, parallel plate colony structure of alpha and beta phases appears only after treatment at 900°C — Fig. 10. The slight reduction in hardness at 700°C seen in Fig. 11, appears to indicate that overaging effects are just beginning to occur at 700°C. Overaging, of course, is the dominant effect in the 900°C treatment, leading to: 1) substantial intragranular coarsening and thicker, grain boundary alpha (Fig. 8), 2) a near-equilibrium alpha-beta plate structure within the grains (Fig. 10), and 3) the highest fusion zone ductility attained in the current investigation.

## Fracture Toughness

Fracture toughness test results appear in Table 3. The results from corresponding SEM observations of the fracture faces are shown in Figs.12–15. All these fractographs were obtained from the stable crack growth region which follows the fatigue precracked zone.

It is apparent that the as-welded condition in all three cases is characterized by a higher fracture toughness than that of the base material. While postweld heat treatment at 900°C has resulted in a further increase in fracture toughness, the treatment at 700°C has led to a substantial reduction in toughness. The latter result was somewhat unexpected and, as mentioned previously, led to a further series of fracture toughness tests employing the single specimen technique. It is noteworthy that the results of the single specimen tests not only matched those of the multiple specimen tests, in general, but also confirmed the inferiority of the 700°C postweld heat treated material, in particular.

The higher fracture toughness of the as-welded fusion zone in relation to the base metal is no doubt due to the fully acicular microstructure, despite a larger prior-beta grain size. The base metal microstructure, on the other hand, is a mixture of equiaxed primary alpha and transformed-beta regions — Fig. 4. It has been known for a long time that beta-processed, plate-like microstructures possess a greater resistance to crack propagation than alpha-beta processed microstructures containing equiaxed alpha. This is valid, as mentioned earlier, for both transgranular and intergranular fractures.

The scanning electron fractographs of the base metal obtained after $J_{IC}$ testing are shown in Fig. 12. Though the higher magnification photograph shows dimples of a wide range of sizes and areas of tearing that are characteristic of ductile fracture, the lower magnification picture reveals a relatively flat fracture face with only minor deviations in crack path. In contrast, fractographs of the as-welded fusion zone shown in Fig. 13 reveal much larger diversions in fracture path as the crack progresses. These predominantly transgranular fractures show vertical faces (Fig. 13A) that are tear ridges. The surfaces are covered with voids and the pictures at higher magnification (Fig. 13, B and D) show dimples surrounded by tear ridges. The relatively high fracture toughness of the weld metal in relation to the base metal, despite the presence of larger prior-beta grains, is thus attributable to the longer path taken by the propagating crack, as evidenced by the rougher fracture topography.

On postweld heat treatment at 700°C, the fracture toughness suffers a drastic reduction from the as-welded value. The scanning electron fractographs (Fig. 14) show a mixture of transgranular and intergranular fracture. Microstructurally, two features are important, as seen in Fig. 7: the intragranular coarsening, which at this temperature is not pronounced, and the grain boundary alpha layer, which also has not developed to any significant thickness. From the fracture toughness viewpoint, the presence of the grain boundary alpha layer is likely to promote intergranular fracture, as the grain boundaries are known to offer ideal sites for void formation (Ref. 12). The fact that the intergranular alpha phase — though softer than the transformed/aged beta structure — is very thin, means that it will be constrained by the surrounding material and cannot easily undergo preferential deformation. The energy required for intergranular crack propagation is thus effectively reduced.

In the case of transgranular fracture, on the other hand, the attendant poor energy absorption is probably due to the

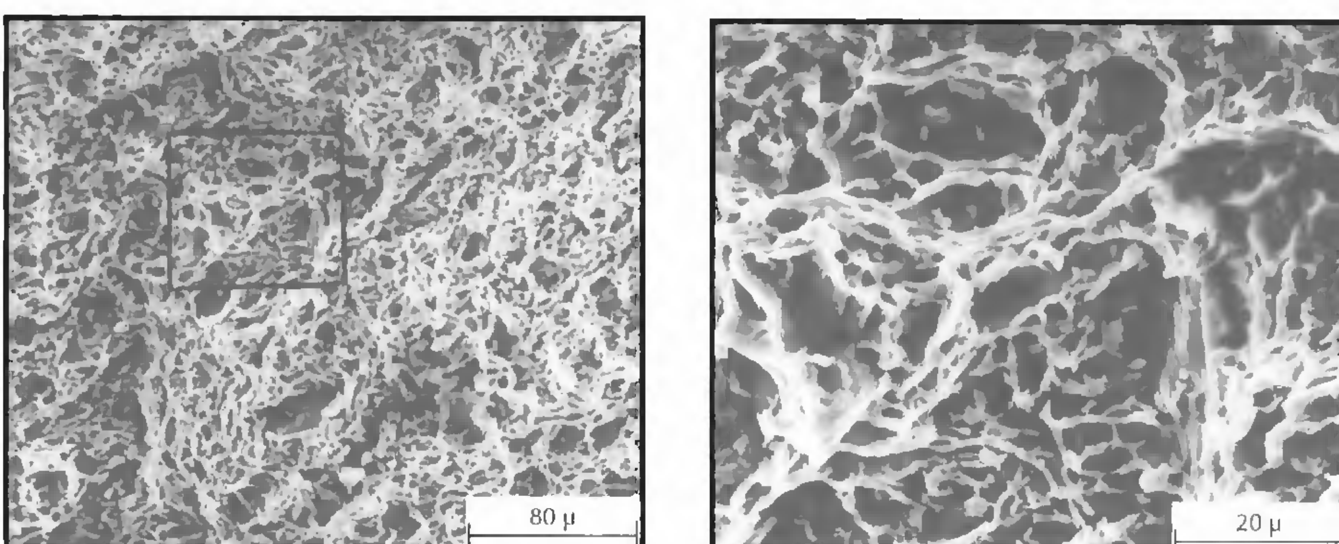


*Fig. 12 — Scanning electron fractographs of Ti-6Al-4V base metal fracture toughness sample.* [Box in (A) magnified in (B).]

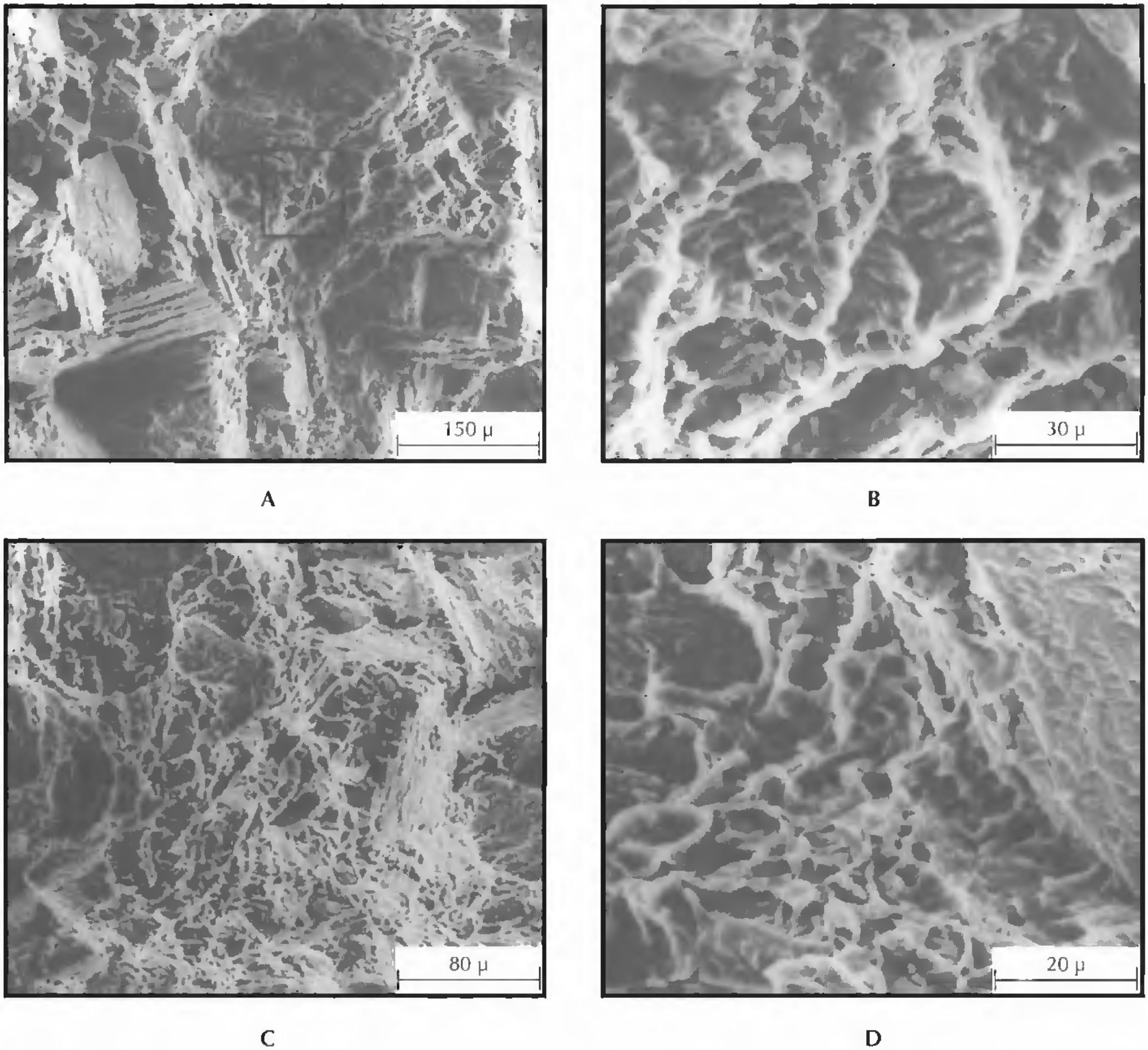


*Fig. 13 — Scanning electron fractographs of fusion zone fracture toughness sample, as-welded condition. A, B — Electron beam weld; C, D — manual GTA weld.* [Box in (A) magnified in (B), (C) and (D) from different regions.]

relatively fine size of the intragranular alpha plates. As discussed earlier, lamellar structures are known to possess fracture toughness superior to that of structures containing equiaxed alpha. It may be further expected that, within the former category, basketweave structures will be tougher than colony structures exhibiting long, straight alpha-beta interfaces. It has, however, been suggested often that such lamellar microstructures should be sufficiently coarse in order to effectively raise fracture toughness. The intragranular alpha plates must be thick enough (large interlamellar spacing) to turn a propagating crack, but short enough and close enough together (smaller colony size) to cause frequent changes in crack growth direction (Ref. 8). It is surmised that, after the heat treatment at 700°C, the intragranular alpha plate thickness has developed only to a small extent so that it is not able to divert a propagating crack. Figure 14 shows little evidence for either plastic flow or crack deviation. Even at higher magnification, only very few dimples can be seen either in the intergranular or the transgranular part. Though there is some evidence of tearing, the fracture appears to be predominantly of the cleavage type. The presence of some secondary cracks on the fracture face can also be noticed in Fig. 14.

The question arises as to why the fracture toughness after the 700°C treatment is lower than in the as-welded condition, which is characterized by an even finer and harder intragranular structure. This, in part, is attributable to the fact that an appreciable fraction of the fracture path in the heat treated material is intergranular and, as explained above, the thin, continuous alpha layer at the grain boundary offers little resistance to crack propagation. The opinion has also been expressed that thin parallel plate morphologies with high aspect ratios (as in the 700°C heat treated material) result in high stress concentration factors and hence low impact toughness (Ref. 22). In support, a nearly identical microstructure, produced in a Ti-6Al-4V alloy by beta-quenching followed by annealing at

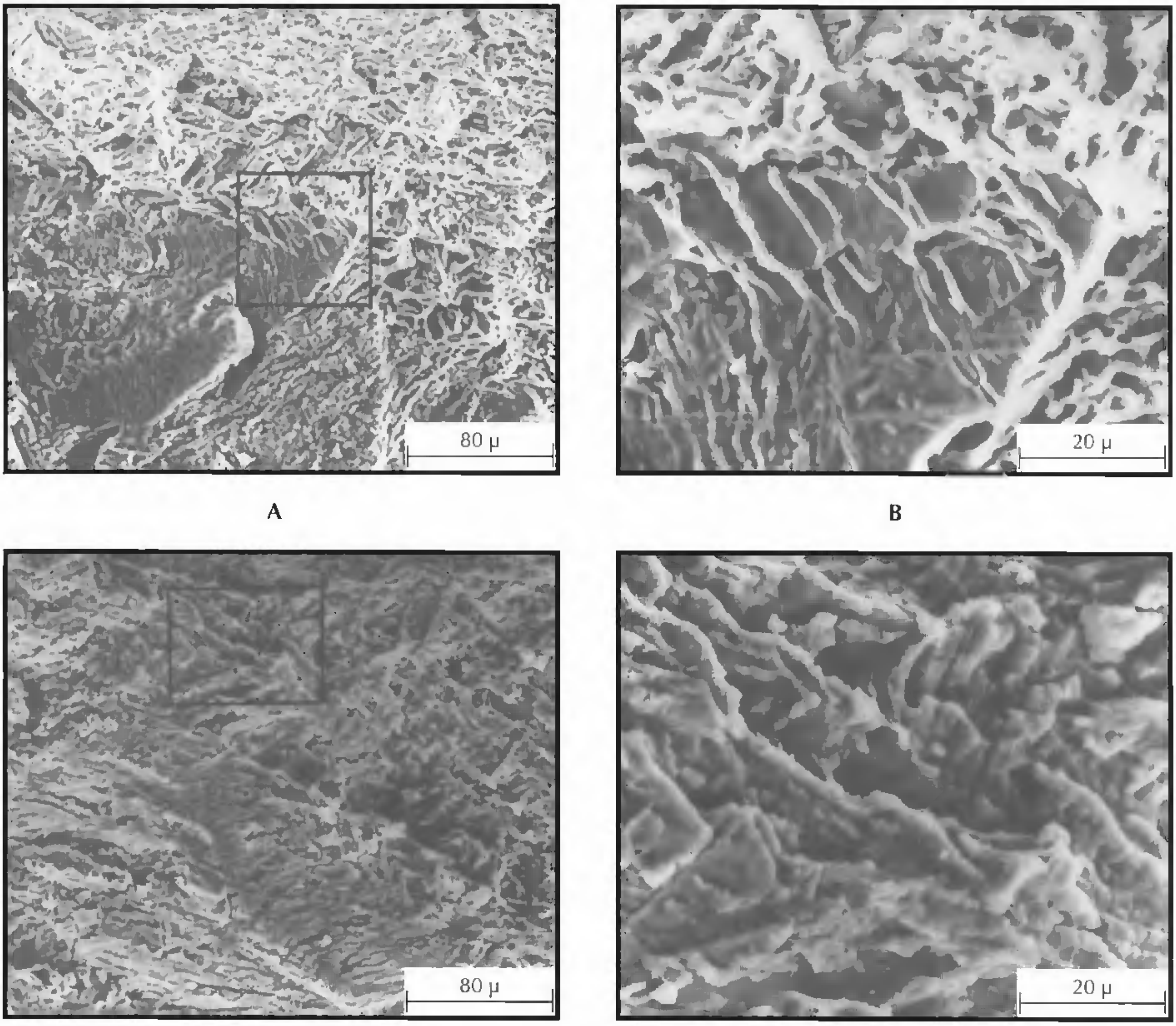


A B C D

*Fig. 14 — Scanning electron fractographs of fusion zone fracture toughness sample after postweld heat treatment at 700°C. A, B — Electron beam weld; C, D — manual GTA weld.* [Boxes in (A) and (C) magnified in (B) and (D), respectively.]

705°C (1301°F), exhibits a fracture toughness even lower than that of the alpha-beta processed and annealed material with a partially equiaxed structure (Ref. 6). A similar lowering of toughness, due in part to the refinement of the alpha-beta colony structure caused by trace additions of boron, has been reported in a Ti-6Al-2Nb-1Ta-0.8Mo alloy (Ref. 23).

Postweld heat treatment at 900°C results in the highest fracture toughness obtained in the present investigation. The microstructure shows a typical basketweave pattern of coarsened alpha plates separated by strips of beta as seen in Fig. 8. The transmission electron micrograph (Fig. 10) shows that the alpha plates have grown to a much larger width than after the treatment at 700°C. An additional feature of the microstructure is the grain boundary alpha layer, which is discontinuous and considerably thicker than that developed by the heat treatment at 700°C.

The fracture surfaces (Fig. 15) show a mixture of well-defined intergranular rupture along prior-beta grain boundaries together with isolated regions of transgranular fracture. The latter regions exhibit strong evidence of ductility in the form of tearing and void formation, with Fig. 15D showing a range of dimple sizes and shapes. That the intergranular part of the fracture is also ductile and involves microvoid coalescence is revealed in the higher magnification picture — Fig. 15F.

The fracture toughness after the 900°C treatment is, on the average, more than double the values obtained after postweld heat treatment at 700°C. It is most likely that this difference arises from the coarser intragranular structure and the thicker grain boundary alpha phase developed at 900°C in relation to that produced at 700°C — Figs. 7 and 8. Considering the transgranular part of the fracture, one may expect that the thicker alpha plates in the intragranular basketweave structure resulting from the 900°C treatment can cause changes in crack path more easily than the thinner platelets developed at 700°C. Crack front deviations can thus occur frequently in the structure produced after

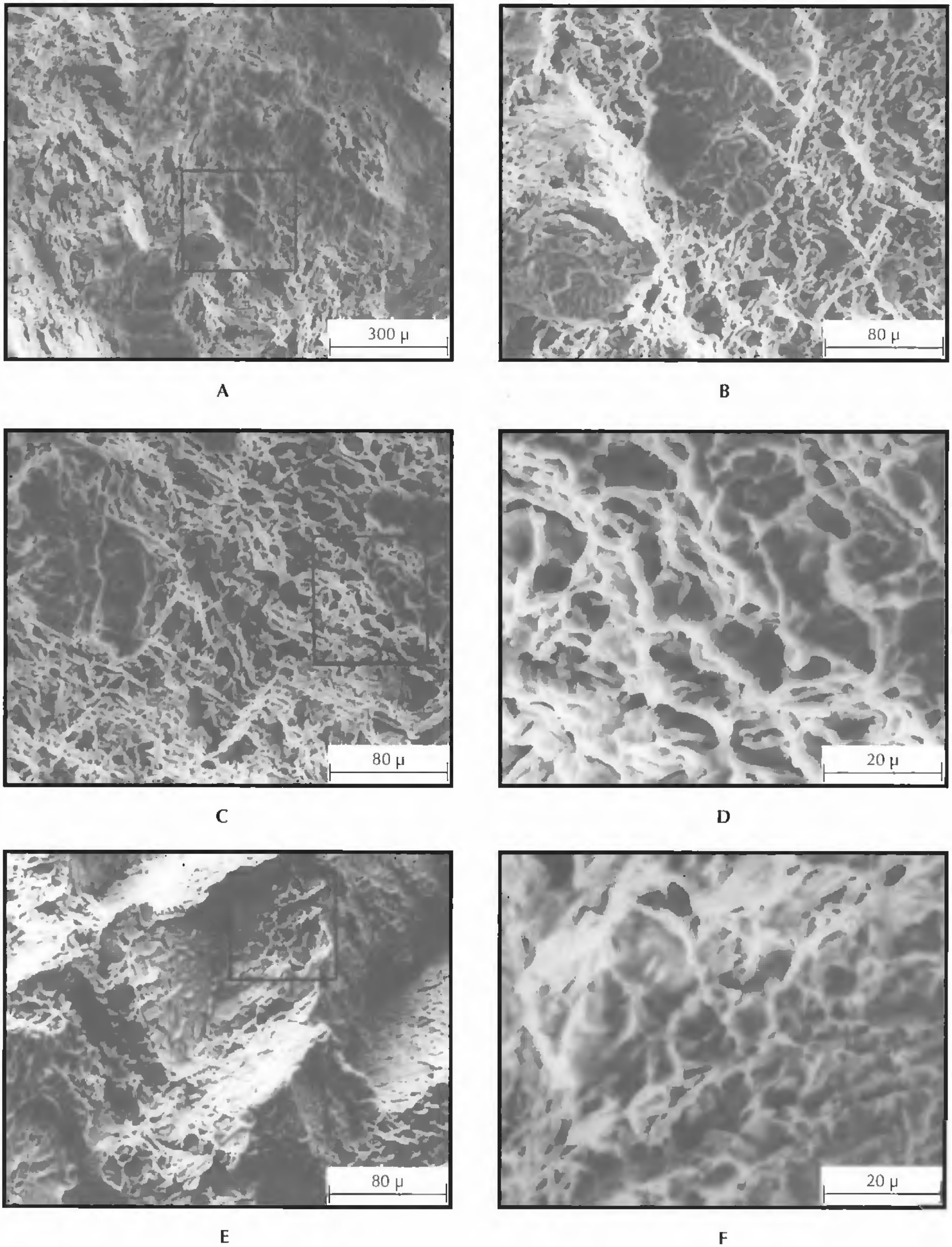


*Fig. 15 — Scanning electron fractographs of fusion zone fracture toughness sample after post-weld heat treatment at 900°C. A, B — Electron beam weld. C, D — Manual GTA weld. E, F — automatic GTA weld.* [Boxes in (A), (C), and (E) magnified in (B), (D), and (F), respectively.]

the higher temperature heat treatment. A comparison of Figs. 14A and 14C with Figs. 15A and 15B and the higher magnification fractograph Fig. 14D with Fig. 15D, clearly reveals that the transgranular portion of the fracture after the 700°C treatment is flatter and shows less evidence of ductility than was shown after the 900°C treatment.

Regarding the intergranular portions of the fracture, the thicker, partially globular grain boundary alpha developed at 900°C also contributes to fracture toughness, since a greater degree of plastic flow can preferentially occur in the thicker alpha phase, which suffers little from the constraining influence of the harder neighboring intragranular structure. This agrees with earlier observations of the role of the intergranular alpha phase, such as, for example, that of Greenfield and Margolin (Ref. 11), who showed that the presence of thicker grain boundary alpha increased the energy required for fracture.

## Conclusions

1) Autogenous fusion welding of an alpha-beta Ti-6Al-4V alloy reduces its ductility but raises the fracture toughness in the as-welded condition. The increase in fracture toughness is attributable to a lamellar intragranular microstructure and the absence of continuous alpha films at the grain boundaries.

2) Postweld heat treatment at 900°C/4 h improves fusion zone ductility and further increases fracture toughness.

3) The temperature of heat treatment should be high in the alpha-beta region, close to the beta-transus. A lower temperature heat treatment at 700°C is detrimental, since it reduces fracture toughness from the as-welded level.

4) The changes in fracture toughness can be related to the morphology and size of the different microstructural constituents, especially grain boundary alpha and intragranular alpha. The highest toughness is exhibited by a coarse, lamellar intragranular structure with discontinuous, globular alpha along the prior-beta grain boundaries.

*Acknowledgment*

The work reported is part of a larger project sponsored by the Department of Science and Technology (India), whose support is gratefully acknowledged.

*References*

1. Baeslack, W. A. III, Becker, D. W., and Froes, F. H. 1984. Advances in titanium alloy welding metallurgy. *Journal of Metals*, 36(5): 46–58.

2. Baeslack, W. A. III, and Banas, C. M. 1981. A comparative evaluation of laser and gas tungsten arc weldments in high-temperature titanium alloys. *Welding Journal*, 60(7): 121-s to 130-s.

3. Baeslack, W. A. III 1982. Technical Note: Evaluation of triplex postweld heat treatments for alpha-beta titanium alloys. *Welding Journal*, 61(6): 198-s to 199-s.

4. Liu, P. S., Baeslack, W. A. III, and Hurky, J. 1994. Dissimilar alloy laser beam welding of titanium: Ti-6Al-4V to Beta-C. *Welding Journal*, 73(7): 175-s to 181-s.

5. Harrigan, M. J. 1982. Effect of chemistry and heat treatment on the fracture properties of Ti-6Al-4V alloy. *Titanium and Titanium Alloys — Source Book*, American Society for Metals: 50–79.

6. Chesnutt, J. C., Rhodes, C. G., and Williams, J. C. 1982. Relationship between mechanical properties, microstructure and fracture topography in alpha-beta titanium alloys. *Titanium and Titanium Alloys — Source Book*, American Society for Metals: 100–139.

7. Williams, J. C., Chesnutt, J. C., and Thompson, A. W. 1987. The effects of microstructure on ductility and fracture toughness of alpha-beta titanium alloys. *Microstructure, Fracture Toughness and Fatigue Crack Growth Rate in Titanium Alloys*, Proc. TMS – AIME Annual Symposium, Denver: 255–270.

8. Stubbington, C. A. 1982. Metallurgical aspects of fatigue and fracture in titanium alloys. *Titanium and Titanium Alloys — Source Book*, American Society for Metals: 140–158.

9. Greenfield, M. A., Pierce, C. M., and Hall, J. A. 1973. The effect of microstructure on the control of mechanical properties in alpha-beta titanium alloys. *Titanium Science and Technology*, AIME: 1732–1743.

10. Margolin, H., Greenfield, M. A., and Greenhut, I. 1973. Yield strength, microstructure and fracture toughness. *Titanium Science and Technology*, AIME: 1709–1717.

11. Greenfield, M. A., and Margolin, H. 1971. The interrelationship of fracture toughness and microstructure in a Ti5.25Al-5.5V-0.9Fe-0.5Cu alloy. *Metallurgical Transactions*, 2(3): 841–847.

12. Rogers, D. H. 1973. The effects of microstructure and composition on the fracture toughness of titanium alloys. *Titanium Science and Technology*, AIME: 1719–1729.

13. Wu, K. C. 1981. Correlation of properties and microstructure in welded Ti-6Al-6V-2Sn. *Welding Journal*, 60(11): 219-s to 226-s.

14. Baeslack, W. A. III, and Mullins, F. D. 1981. Relationship of mechanical properties to microstructure and fractographic features in a welded high toughness titanium alloy. *Proceedings of the ASM: Trends in Welding Research in the United States*, 541–560.

15. Topolskii, V. F., *et al.* 1975. Properties of joints in VT6 alloy after welding and heat treatment. *Automatic Welding*, 6: 48–51.

16. Zagrebenyuk, S. D., *et al.* 1974. Effect of welding conditions on the properties of welded joints in high temperature titanium alloy VT9. *Welding Production*, 6: 37–39.

17. Gurevich, S. M., *et al.* 1973. Weldability of titanium alloy AT3. *Welding Production*, 11: 33–36.

18. Esina, D. I., *et al.* 1983. Fracture toughness of welded joints in VT6S and AT6 titanium alloys. *Automatic Welding*, 6: 44–46.

19. Borggreen, K., and Wilson, I. 1980. Use of postweld heat treatment to improve ductility in thin sheets of Ti-6Al-4V. *Welding Journal*, 59(1): 1-s to 9-s.

20. Standard test method for $J_{IC}$, a measure of fracture toughness, ASTM: E813-89, American Society for Testing and Materials: 713–727.

21. Baker, T. S. 1986. Effect of stress relief on fatigue crack propagation and fracture toughness of laser beam welded 4 mm thick Ti-6Al-4V alloy sheet. *Proceedings of Conference for Designing Titanium*, Bristol, UK: 267–276.

22. Khorev, M. A., *et al.* 1981. The mechanical properties and structure of electron beam welded joints in the VT23 titanium alloy. *Welding Production*, 7: 19–22.

23. Inouye, H., and David, S. A. 1984. Segregation and influence of boron on the impact toughness of Ti-6Al-2Nb-1Ta-0.8Mo welds and castings. Met. Trans, 15A(7): 1505–1507.